iScience

CellPress

Article

Functional Interaction of BRCA1 and CREBBP in Murine Hematopoiesis

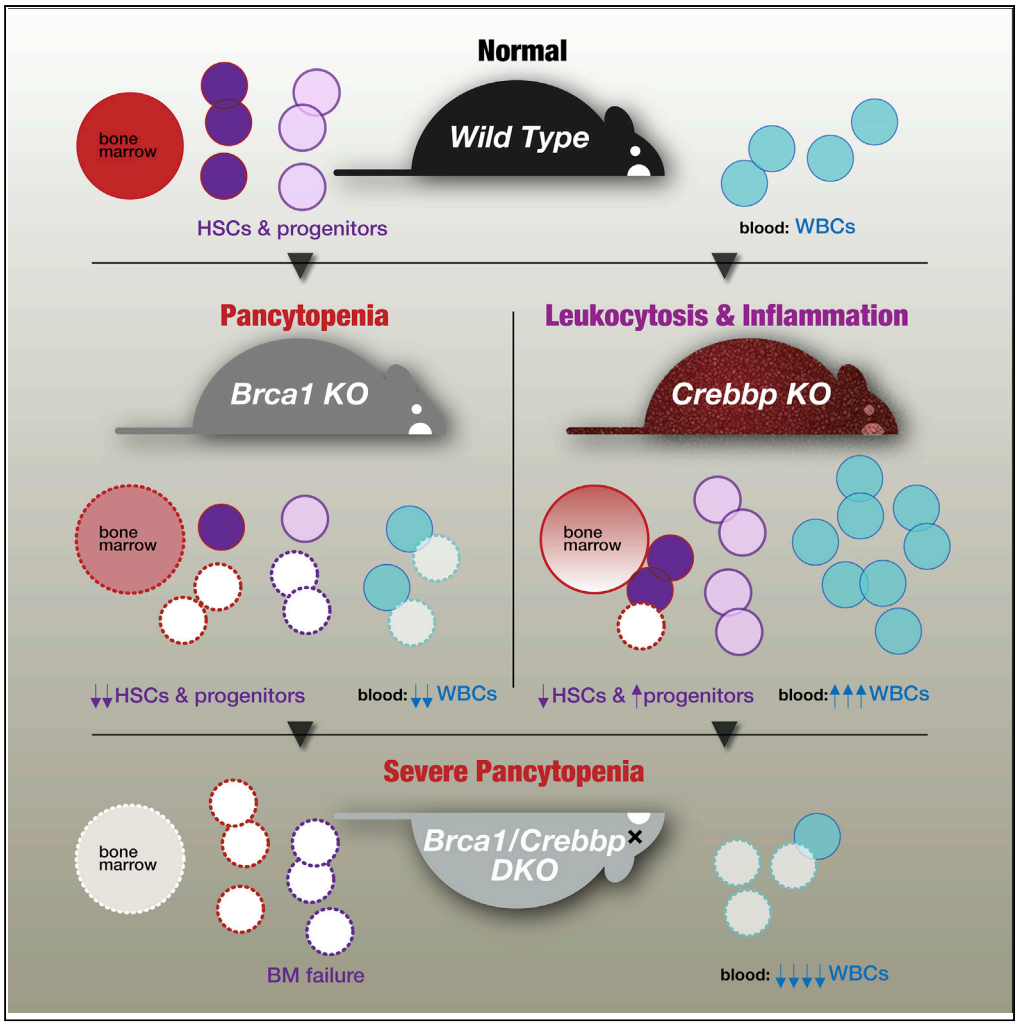

Sam R. Holmstrom, Ranjula Wijayatunge, Kelly McCrum, Victoria E. Mgbemena, Theodora S. Ross

theo.ross@utsw.edu

HIGHLIGHTS

Crebbp deficiency leads to an inflammatory condition including a lethal dermatitis

Brca1 and *Crebbp* co-deletion leads to rapid bone marrow failure and lethality

Brca1 protein levels are diminished in thymic tissue from Crebbp-deficient mice

Holmstrom et al., iScience *19*, 809–820
September 27, 2019
https://doi.org/10.1016/j.isci.2019.08.031

iScience

CellPress

Article

Functional Interaction of BRCA1 and CREBBP in Murine Hematopoiesis

Sam R. Holmstrom,[1,2] Ranjula Wijayatunge,[1,2] Kelly McCrum,[1] Victoria E. Mgbemena,[1] and Theodora S. Ross[1,3,*]

SUMMARY

Both BRCA1 and CREBBP are tumor suppressor genes that are important for hematopoiesis. We have previously shown that mouse *Brca1* is essential for hematopoietic stem cell (HSC) viability. In contrast to *Brca1* deficiency, which results in pancytopenia, we report here that *Crebbp* deficiency results in myeloproliferation associated with an increase of splenic HSCs as well as a lethal systemic inflammatory disorder (LD50 = 86 days). To investigate the interaction of these two proteins in hematopoiesis, we generated double *Crebbp/Brca1* knockout mice (DKOs). To our surprise, DKOs had accelerated bone marrow failure compared with *Brca1*-deficient mice and this was associated with an even shorter lifespan (LD50 = 88.5 versus 33 days). Furthermore, *Crebbp* or *Brca1* heterozygosity influenced the hematopoietic phenotype associated with complete deficiency of *Brca1* or *Crebbp*, respectively. We also observed lower BRCA1 protein levels in hematopoietic tissues when CREBBP is absent. Collectively, these data suggest *Crebbp* and *Brca1* functionally interact to maintain normal hematopoiesis.

INTRODUCTION

BRCA1 and *CREB-Binding protein (CREBBP or CBP)* are tumor suppressor genes that are important in normal development. Homozygous germline mutations in either of these genes are embryonic lethal in humans and mice. In humans, heterozygous germline *CREBBP* mutations cause Rubenstein-Taybi Syndrome, a developmental disorder (short stature, intellectual disability, etc.) that includes a predisposition to leukemia (Miller and Rubinstein, 1995; Schorry et al., 2008). Unlike *CREBBP* mutations, *BRCA1* mutations do not predispose humans to hematopoietic neoplasia but do predispose to other solid tumors, such as pancreatic and prostate cancers, in addition to breast and ovarian cancers (Futreal et al., 1994; Miki et al., 1994).

Mice haploinsufficient for *Crebbp* develop myeloproliferative disorders and myelodysplastic syndromes by 1 year of age, which can progress to full-blown malignancies (Kung et al., 2000; Zhou et al., 2016; Zimmer et al., 2012). Complete deletion of *Crebbp* in hematopoietic stem cells (HSCs) impairs T and B cell development (Kasper et al., 2006; Xu et al., 2006) and increases differentiation to granulocytic and monocytic lineages (Chan et al., 2011). In addition, either mono- or biallelic loss of Crebbp in bone marrow is reported to impair the self-renewing capacity of HSCs (Chan et al., 2011; Rebel et al., 2002).

Although *BRCA1* mutations do not predispose mice to leukemia, mice conditionally deficient for *Brca1* in embryonic HSCs develop a severe pancytopenia and die within 3 months of age (Mgbemena et al., 2017). This is quite different from mice conditionally deficient for *Brca1* in adult HSCs and progenitors using Mx1-Cre activation, which leads to a modest reduction in HSCs and mild bone marrow dysfunction (Vasanthakumar et al., 2016).

Although *Crebbp* and *Brca1* are both required to preserve normal HSC pools in bone marrow, their individual deficiencies result in distinct consequences (Chan et al., 2011; Kung et al., 2000; Mgbemena et al., 2017; Vasanthakumar et al., 2016; Zimmer et al., 2012). To investigate functional interactions of *Brca1* and *Crebbp* in hematopoiesis, we co-deleted both genes in HSCs and progenitors using the hematopoietic system-specific Vav1-iCre (Georgiades et al., 2002). Unexpectedly, we found that *Crebbp*-deficiency phenotypes are dependent on the presence or absence of *Brca1*. *Crebbp* deficiency in the background of normal *Brca1* led to leukocytosis and neutrophilia, whereas co-deletion of *Crebbp* with *Brca1* led to a more severe pancytopenia than that found for *Brca1* deficiency alone. We also show that, in contrast to previous studies (Chan et al., 2011; Zimmer et al., 2011, 2012), hematopoietic loss of *Crebbp* alone resulted in a shift in the balance of HSCs where the decrease in the bone marrow was made up for in an increase in the spleen, rather than an overall shortage of HSCs. Furthermore, *Crebbp* heterozygosity showed enhanced

[1]Department of Internal Medicine, University of Texas Southwestern Medical Center, ND3.214, 5323 Harry Hines Boulevard, Dallas, TX 75390, USA

[2]These authors contributed equally

[3]Lead Contact

*Correspondence: theo.ross@utsw.edu

https://doi.org/10.1016/j.isci.2019.08.031

hematopoietic defects in young mice with *Brca1*-deleted bone marrow, whereas *Brca1* heterozygosity showed mild attenuation of pathogenic consequences in *Crebbp*-deficient mice. Further support for a functional interaction between BRCA1 and CREBBP was found where BRCA1 levels were altered in *Crebbp*-deficient thymus and bone marrow-derived macrophages (BMDMs), adding support that these two genes cooperate *in vivo*.

RESULTS

Deficiency of *Crebbp* in Mouse Hematopoietic Tissue Leads to an Inflammatory Disorder

We, and others, have discovered that deletion of *Brca1* in HSCs results in either hematopoietic failure by 1 month of age when deleted in embryonic HSCs or a moderate reduction in bone marrow function when deleted in adult HSCs (Mgbemena et al., 2017; Vasanthakumar et al., 2016). *Crebbp* has also been shown to contribute to maintenance of normal levels of early progenitors (Kung et al., 2000). Since *Brca1* and *Crebbp* are important in hematopoiesis, we tested the functional interaction of these genes in knockout mice. Specifically, we conditionally deleted *Crebbp* alone or with *Brca1* using the early hematopoietic system-specific Vav1-iCre (Georgiades et al., 2002) and compared them with previously described Vav1-iCre;*Brca1*$^{F/F}$ mice (Mgbemena et al., 2017).

Vav1-iCre;*Crebbp*$^{F/F}$ mice survived a median 86 days (Figure 1A), and their mortality was associated with an unexpected severe skin phenotype (Figure 1B). This included skin flaking that began at 4–5 weeks of age with alopecia in the tail, eyelids, and ears. This progressed to widespread alopecia, flaking, and ulceration by 3–4 months of age. Once severe dermatitis developed, mice became moribund and were euthanized. Similar to age-matched controls (Figure 1C), skin from young pre-symptomatic Vav1-iCre;*Crebbp*$^{F/F}$ mice showed normal epidermal structure (Figure 1D, left). However, higher magnification showed abnormal granulocyte infiltration (black arrows) in the dermal layers (Figure 1D, right). Compared with normal skin structure in adult mice (Figure 1E), diseased Vav1-iCre;*Crebbp*$^{F/F}$ adult mice showed significant epidermal hyper-proliferation and a fibrotic dermal layer (Figure 1F, left) with granulocytes (black arrows) and mast cells (white arrow) (Figure 1F, right). Unlike biallelic *Crebbp*-deficient mice, heterozygous Vav1-iCre;*Crebbp*$^{F/+}$ mice showed long-term survival and did not have skin abnormalities during their lifespan (data not shown).

Young Vav1-iCre;*Crebbp*$^{F/F}$ mice also showed lung inflammation (Figure 1H, left). Higher magnification (Figure 1H, right) showed localized plasma cell accumulations (hatched arrow) and pockets of foamy macrophages (white arrow) that accompanied granulocyte infiltration (black arrows). Immune cell infiltration persisted in lungs of older diseased Vav1-iCre;*Crebbp*$^{F/F}$ mice (Figure 1J, left), with frequent Immunoglobulin-rich Russell bodies (orange arrows) in plasma cell-dense regions (hatched arrow) of the lungs (Figure 1J, right). Representative WT lungs from young (Figure 1G) and adult (Figure 1I) mice are shown for comparison.

Similar to other *Crebbp*-deficiency studies (Kung et al., 2000; Zhou et al., 2016; Zimmer et al., 2012), Vav1-iCre;*Crebbp*$^{F/F}$ mice developed splenomegaly (Figure 2A). Compared with controls *Crebbp*-deficient spleens were enlarged as early as 1 month of age (1.2% of body weight versus 0.5% body weight in control, $p < 0.0001$) (Figure 2A, left) and by adulthood (Figure 2A, right) had ~6-fold greater spleen weight than littermate controls (2.7% of body weight in *Crebbp*-deficient mice compared with 0.5% in controls, $p < 0.01$). In contrast to splenomegaly, bone marrow cellularity in Vav1-iCre;*Crebbp*$^{F/F}$ mice was similar to controls (Figure S1A).

Compared with age-matched controls (Figures 2B and 2C), H&E stains from young and adult Vav1-iCre;*Crebbp*$^{F/F}$ mice (Figures 2D and 2E) showed age-related progression of extramedullary hematopoiesis in red pulp with concomitant depletion of lymphoid structure in white pulp.

In parallel with the inflammatory phenotype, Vav1-iCre;*Crebbp*$^{F/F}$ mice had leukocytosis. Elevated white blood cells (WBCs) (Figure 2F) were present in young *Crebbp*-deficient mice (4–8 weeks) and persisted throughout adulthood (8–24 weeks) (gray circles). The WBC differential showed Vav1-iCre;*Crebbp*$^{F/F}$ mice had neutrophilia, monocytosis, and eosinophilia, with neutrophils increasing with age (Figures 2G–2I). Lymphocyte counts were normal (Figure 2J). In contrast to the previous reports of Mx1-Cre-mediated deletion of *Crebbp* in adulthood (Chan et al., 2011), we did not observe thrombocytopenia in Vav1-iCre;*Crebbp*$^{F/F}$ mice (Figure S1B). Both young and adult *Crebbp*-deficient mice were anemic (Figures 2K–2M).

HSC frequencies ($CD150^+CD48^-Lineage^-Sca\text{-}1^+ckit^+$;$CD150^+CD48^-$LSK) (Kiel et al., 2005) in bone marrow from 4- to 8-week-old Vav1-iCre;*Crebbp*$^{F/F}$ mice were lower compared with age-matched littermate

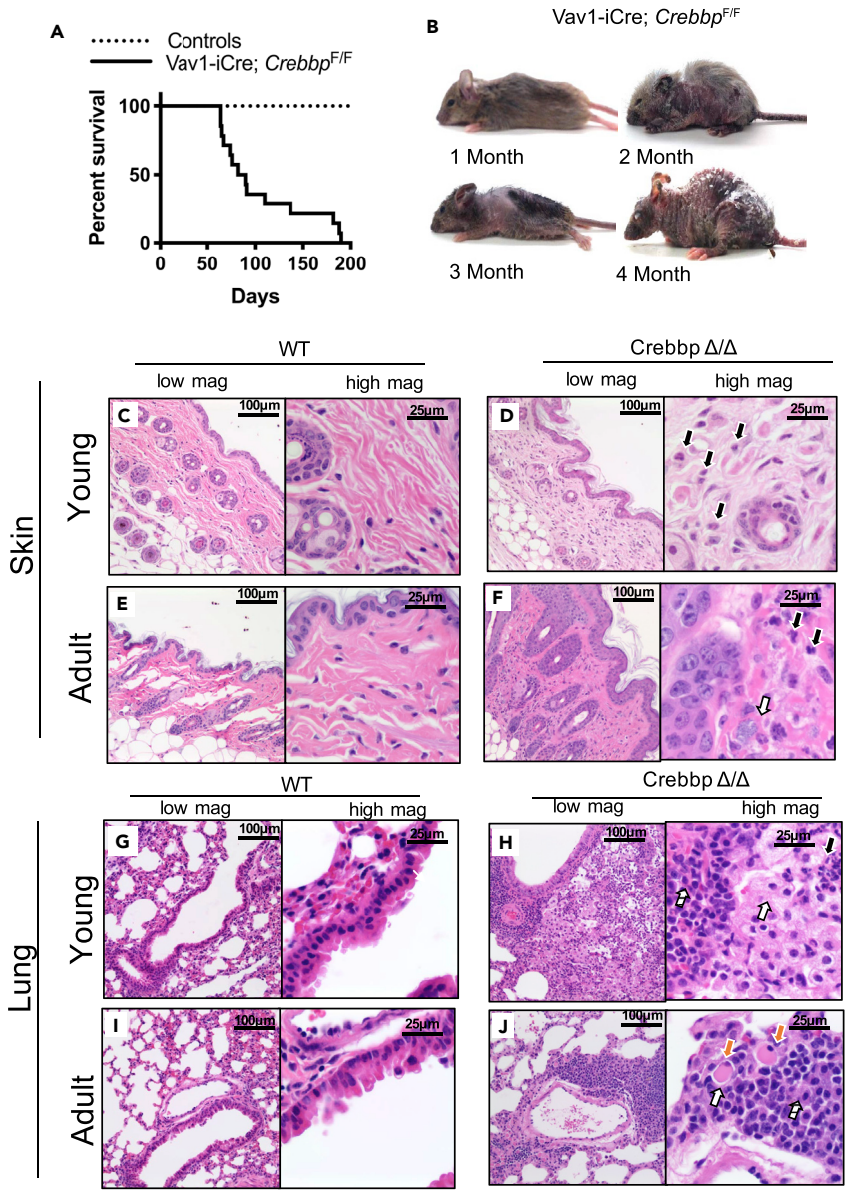

Figure 1. Deficiency of *Crebbp* in Mouse Hematopoietic Tissue Leads to an Inflammatory Disorder

(A and B) (A) Kaplan-Meier curves show that mice with hematopoietic deletion of *Crebbp* (Vav1-iCre;*Crebbp*$^{F/F}$) experienced early lethality (LD50 = 86 days, n = 14) that was associated with a systemic inflammatory disorder that progressed to (B) severe ulcerative dermatitis by 3–4 months of age.

(C–I) (C) Representative H&E stains of skin cross sections from young (~6 weeks) (C) WT and (D) Vav1-iCre;*Crebbp*$^{F/F}$ and adult (~4 months) (E) WT and (F) diseased Vav1-iCre;*Crebbp*$^{F/F}$ mice (left [low magnification] and right [high magnification] panels). (D) Young Vav1-iCre;*Crebbp*$^{F/F}$ had dermal granulocyte infiltration (right panel, black arrow) with normal epidermis. (F) Adult *Crebbp*-deficient mice had epidermal hyper-proliferation and immune infiltration of the dermis including mast cells (right panel, white arrow) and granulocytes (right panel, black arrow). Compared with (G) young and (I) adult WT lungs, (H) young Vav1-iCre;*Crebbp*$^{F/F}$ lungs had foamy macrophages (white arrow), granulocytes (black arrow), and plasma cell accumulation (hatched arrow).

(J) Adult Vav1-iCre;*Crebbp*$^{F/F}$ had frequent Russell bodies (orange arrow) within plasma cell accumulations (right panel, hatched arrow).

Abbreviations: WT, wild-type; *Crebbp*$^{\Delta/\Delta}$, Vav1-iCre;*Crebbp*$^{F/F}$.

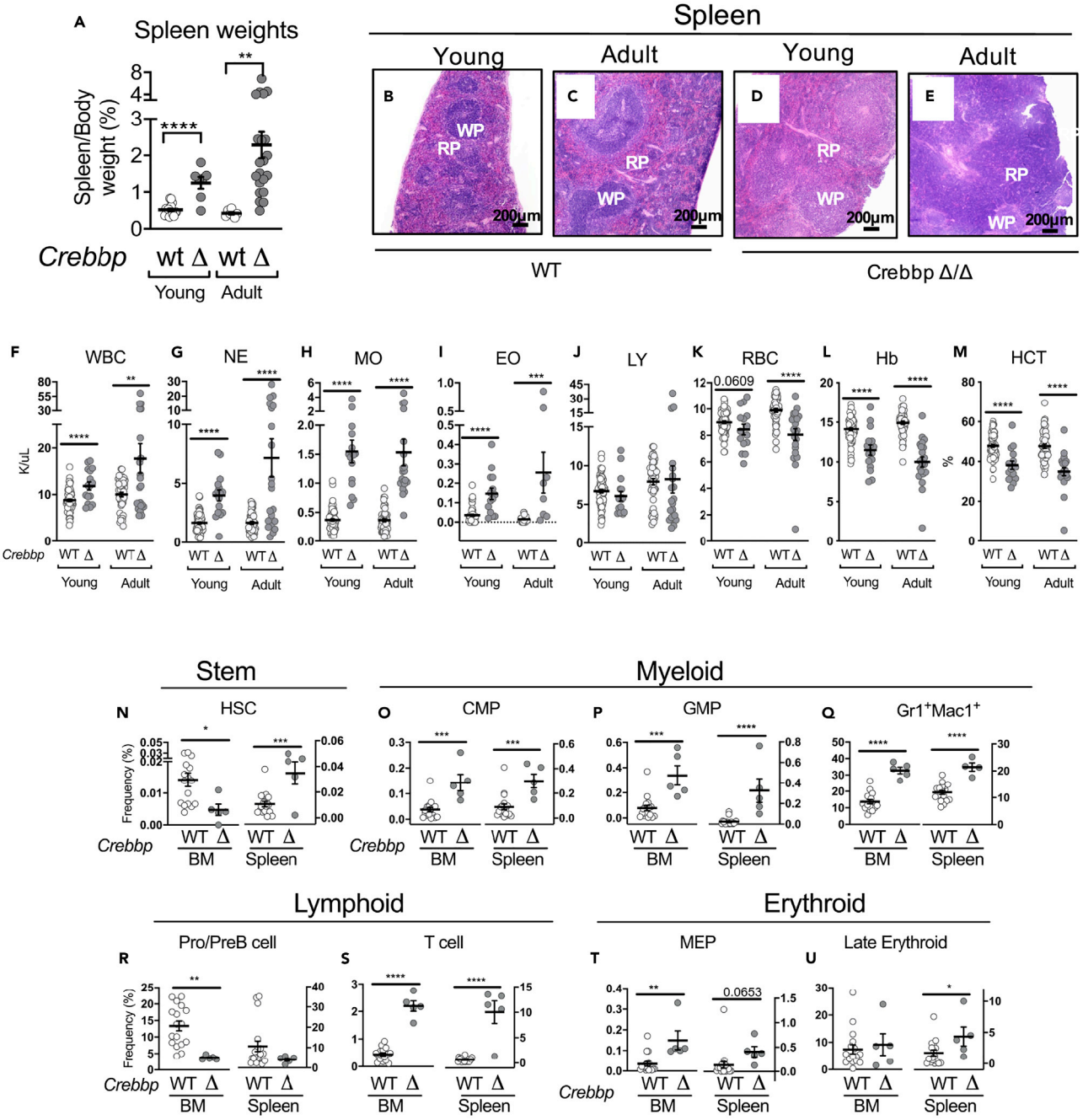

Figure 2. Early Hematopoietic Deletion of *Crebbp* Leads to Leukocytosis

(A–M) (A) Vav1-iCre;*Crebbp*$^{F/F}$ mice (gray circles) had enlarged spleens (% body weight) compared with controls (open circles, Vav1-iCre negative) at 4–8 weeks (young, $p < 0.0001$) and >8–24 weeks (adult $p < 0.01$). Representative H&E stains of spleens from (B) young and (C) adult control mice compared with (D) young and (E) adult Vav1-iCre;*Crebbp*$^{F/F}$ mice had white pulp (WP) depletion and progressive extramedullary expansion in red pulp (RP) of *Crebbp*-deficient mice. Peripheral blood analyses of (F) white blood cells (WBC), (G) neutrophils (NE), (H) monocytes (MO), (I) eosinophils (EO), (J) lymphocytes (LY), (K) red blood cells (RBC), (L) hemoglobin (Hb), and (M) hematocrit (HCT) for young (4–8 weeks, n = 16) and adult (>8–24 weeks, n = 22) mice with hematopoietic deletion of *Crebbp* (gray circles, Vav1-iCre;*Crebbp*$^{F/F}$), compared with young (n = 68) and adult (n = 48) matched controls (open circles) showed a myeloid leukocytosis.

(N–U) Flow cytometric analysis of bone marrow (left) and splenic (right) (N) HSCs, (O) CMPs, (P) GMPs, (Q) GMs, (R) B cell progenitors, (S) T cell progenitors, (T) MEPs, and (U) erythroid progenitors for 4- to 8-week-old *Crebbp*-deficient mice (Vav1-iCre;*Crebbp*$^{F/F}$, n = 4–6) (filled gray circles), compared with age-matched littermate controls (clear circles, n = 15). Spleen weight numbers: Vav1-iCre control: young n = 17, adult n = 7; Vav1-iCre:*Crebbp*$^{F/F}$: young n = 7, adult n = 21.

Values represent means ± SEM. Statistical significance was assessed using a two-tailed Student's t test (*$p < 0.05$, **$p < 0.01$, ***$p < 0.001$,****$p < 0.0001$).

controls (Figure 2N, left). Although this finding is consistent with previous reports (Chan et al., 2011), we also noted an increase in splenic HSCs (Figure 2N, right). Both spleen and bone marrow from 4 to 8 week-old *Crebbp*-deficient mice showed higher levels of common myeloid progenitors (CMP, $CD34^{+}CD16/32^{low}$ $CD127^{-}Sca\text{-}1^{-}LK$), myeloid granulocyte/monocyte mid progenitors (GMP; $CD34^{+}CD16/32^{high}$ $CD127^{-}Sca\text{-}1^{-}LK$) (Akashi et al., 2000), and granulocyte/monocyte late progenitors ($Gr1^{+}Mac1^{+}$; $CD11b^{+}Gr1^{+}$) (Figures 2O–2Q), as well as $CD3^{+}$T cell progenitors (Figure 2S). In agreement with previous reports identifying a role for CREBBP in B cell maturation (Xu et al., 2006; Zimmer et al., 2011), loss of *Crebbp* in bone marrow resulted in significantly reduced ProB/PreB-cell frequencies ($CD43^{-}B220^{hi}/B220^{lo}$) in bone marrow (Figure 2R, left) with less of an effect in spleen (Figure 2R, right). The inverse changes in T and B cell progenitor frequencies in *Crebbp*-null mice may explain the lack of net changes in total lymphocyte counts (Figure 2J). Megakaryocyte/erythroid mid progenitors (MEPs; $CD34^{-}CD16/32^{low}CD127^{-}Sca\text{-}1^{-}LK$) (Akashi et al., 2000) were higher in Vav1-iCre;$Crebbp^{F/F}$ bone marrow and spleen, but only splenic late erythroid progenitors were higher (Figures 2T and 2U).

This is the first report of the use of the *Vav-Cre* allele to achieve biallelic deletion of *Crebbp* in adult and embryonic HSCs. These robust phenotypic data (inflammatory disorder, myeloproliferation) complement prior reports of *Crebbp* deficiency phenotypes. The other reports either studied heterozygous germline *Crebbp* knockouts or used the Mx1-Cre allele to achieve biallelic deletion of *Crebbp* in HSCs. For comparison of previous results to the data presented here, we have included a table comparing phenotypes (Table S1).

Brca1 and *Crebbp* Co-deficiency in Hematopoietic Tissue Leads to Increased Mortality due to Severe Bone Marrow Failure

To investigate the functional interaction of *Brca1* and *Crebbp* genes in hematopoietic tissue, we deleted both genes in bone marrow and compared them with each of the single knockouts. To our surprise, Vav1-iCre;$Brca1^{F/F}$;$Crebbp^{F/F}$ (double *Crebbp/Brca1* knockout mice [DKO]) mice died much earlier (LD50 = 33 days) than Vav1-iCre;$Crebbp^{F/F}$ (LD50 = 86 days) or our previously published Vav1-iCre;$Brca1^{F/F}$ mice (LD50 = 88.5 days) (Figure 3A; $p < 0.001$). The detrimental effect of *Brca1/Crebbp* co-deletion was also apparent in our ability to generate only eight DKO mice over 3 years, despite optimal breeding schemes. *Crebbp* loss in the DKO mice did not result in skin abnormalities, possibly because these mice did not survive to an age where severe skin phenotypes in Vav1-iCre;$Crebbp^{F/F}$ mice developed (3–4 months of age). Histology of bone marrow from the DKO mice showed decreased cellularity (Figures 3B and 3C). Bone marrow cell numbers were 80% lower in DKOs compared with control mice (Figure 3D). As expected, DKOs showed absence of bone marrow HSCs (Figure 3E) and loss of most mid and late progenitors (Figure S2). DKOs (open diamonds), like Vav1-iCre;$Brca1^{F/F}$ (downward triangles), developed pancytopenia that was even a more severe than age-matched Vav1-iCre;$Brca1^{F/F}$ mice (Figures 3F–3L). Together, these data show that *Crebbp* and *Brca1* have distinct effects on hematopoiesis, where *Crebbp* restrains aberrant leukocytosis and possible HSC mobilization and also compensates for *Brca1* loss to maintain HSCs/progenitors.

Brca1 and *Crebbp* Gene Dosage Impacts Hematopoiesis

Heterozygous *CREBBP* mutations in humans predispose patients with Rubenstein-Taybi Syndrome to hematopoietic neoplasia (Miller and Rubinstein, 1995; Schorry et al., 2008). Also, *Brca1* heterozygosity has been associated with increased frequency of febrile neutropenia after chemotherapy (Mgbemena et al., 2017). Whether heterozygous mutations in either gene impact other phenotypes is not known. Here, we tested whether the heterozygous states of either *Crebbp* or *Brca1* affected the deficient phenotypes of the other. Combined *Brca1* and *Crebbp* heterozygosity (Vav1-iCre; $Brca1^{F/+}$;$Crebbp^{F/+}$) did not affect survival (Figure 4A, gray line) or CBCs (Figures 4B–4F, open circles versus open squares), except for a mild but significant increase in monocytes (Figure 4E). Mice with *Brca1* heterozygosity combined with complete *Crebbp* deficiency (Vav1-iCre; $Brca1^{F/+}$;$Crebbp^{F/F}$) showed slightly longer survival than Vav1-iCre;$Crebbp^{F/F}$ mice, but this change was not significant (LD50 = 107 versus 86 days, $p = 0.069$) (Figure 4A, dotted versus solid line). However, young Vav1-iCre;$Brca1^{F/+}$;$Crebbp^{F/F}$ mice displayed lower WBC counts ($p < 0.05$) compared with Vav1-iCre;$Crebbp^{F/F}$ mice; individual counts for neutrophils (NE) ($p = 0.073$), monocytes (MO) ($p = 0.06$), and eosinophils (EO) ($p = 0.094$), although lower, were not significant (Figures 4B–4E; gray triangles versus gray circles). *Brca1* heterozygosity in Crebbp-deficient mice led to a decrease of RBC counts (Figure 4G, open circles versus gray triangles).

Brca1 haploinsufficiency in Vav1-iCre; $Brca1^{F/+}$;$Crebbp^{F/F}$ mice (gray triangles) normalized splenic HSCs compared with *Crebbp*-deficient mice (Figure 4H, right; gray circles versus triangles) and attenuated

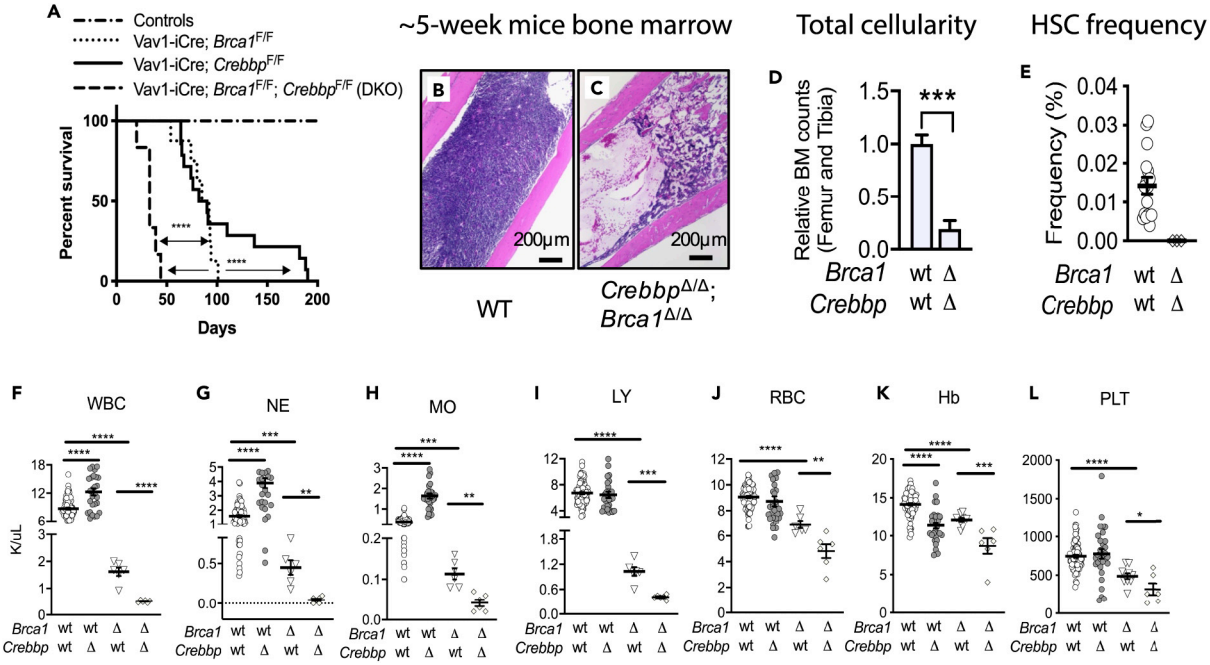

Figure 3. Double Knockout of *Brca1* and *Crebbp* in Hematopoietic Tissues Leads to Rapid Death Associated with Severe Bone Marrow Failure

(A–C) (A) Kaplan-Meier survival analysis shows hematopoietic co-deletion of *Brca1* and *Crebbp* (Vav1-iCre $Brca1^{F/F}$;$Crebbp^{F/F}$, [DKO]) results in greater lethality (LD50 = 33 days, n = 6) than loss of either *Brca1* (Vav1-iCre;$Brca1^{F/F}$, LD50 = 88.5 days, n = 8) or *Crebbp* (Vav1-iCre;$Crebbp^{F/F}$, LD50 = 86, n = 12) alone, compared with littermate control mice (Vav1-iCre negative, n = 9). H&E stains show comparison of (B) normal bone marrow and (C) ablated bone marrow in DKO mice.

(D–L) (D) Quantification of bone marrow counts in long bones (2x femur and tibia) show 80% decrease in cellularity in DKOs (WT, n = 15; DKO, n = 4). Early lethality in DKO mice correlates with (E) ablated HSCs (WT, n = 15; DKO, n = 4) and (F–L) more advanced pancytopenia compared with age-matched (4–8 weeks) mice with only *Brca1* deletion (Vav1-iCre;$Brca1^{F/F}$). Peripheral (F) white blood cells (WBC), (G) neutrophils (NE), (H) monocytes (MO), (I) lymphocytes (LY), (J) red blood cells (RBC), (K) hemoglobin (Hb), and (L) platelets (PLT) are shown from 4- to 8-week-old mice. Blood count numbers: Age-matched litter mate control (Vav1-iCre negative) n = 92 (open circles); Vav1-iCre;$Crebbp^{F/F}$ n = 30 (gray circles); Vav1-iCre;$Brca1^{F/F}$ n = 6 (open downward triangles); DKO n = 6, (open diamonds). Values represent means ± SEM. Statistical significance was assessed using a two-tailed Student's t test except in (A) where a long-rank test was used (*$p < 0.05$, **$p < 0.01$, ***$p < 0.001$, ****$p < 0.0001$).

most bone marrow myeloid progenitors. Except for late granulocyte/monocyte ($Gr1^{+}Mac1^{+}$) progenitors spleen showed similar trends (Figures 4I–4K). In addition, Vav1-iCre;$Brca1^{F/+}$; $Crebbp^{F/F}$ splenic T cells were normalized toward wild-type (WT) frequencies (open circles) (Figure 4L, right). *Brca1* heterozygosity (gray triangles) did not significantly alter *Crebbp*-deficiency-associated ProB/PreB loss in bone marrow (Figure 4M, left). Splenic early erythroid progenitors were unchanged (Figure 4N), whereas late erythroid progenitors were elevated in Vav1-iCre; $Brca1^{F/+}$;$Crebbp^{F/F}$ mice compared with controls (Figure 4O, right), although RBCs were decreased with *Brca1* heterozygosity (Figure 4G). We did observe a mild but insignificant reduction in lifetime incidence of skin abnormalities in Vav1-iCre; $Brca1^{F/+}$;$Crebbp^{F/F}$ compared with Vav1-iCre;$Crebbp^{F/F}$ mice (Figure 4P; p = 0.083, Fisher's exact test).

Hematopoietic abnormalities have been previously reported for *Crebbp* heterozygous mice that appear in late adulthood (>1 year) (Kung et al., 2000). We tested whether a heterozygous *Crebbp* genetic background affected young mice that were *Brca1*-deficient. Although *Crebbp* heterozygosity did not alter lifespan of *Brca1*-deficient mice (Figure 4Q, Vav1-iCre;$Brca1^{F/F}$;$Crebbp^{F/+}$), WBC and neutrophil counts were moderately reduced (Figures 4R and 4S) and RBC counts trended lower (Figure 4T). That *Crebbp* and *Brca1* allele dosage influence the deficiency phenotype of the other is further evidence these two genes cooperate. However, it is not clear whether this cooperation is direct or indirect.

BRCA1 Protein Is Altered in CREBBP-Deficient Hematopoietic Tissues

Since previous data have shown that CREBBP regulates *BRCA1* gene expression (Ogiwara and Kohno, 2012; Pao et al., 2000), we explored whether similar direct relationships were present in hematopoietic tissue. We chose thymus as our model hematopoietic tissue for two reasons: (1) thymus has robust mRNA

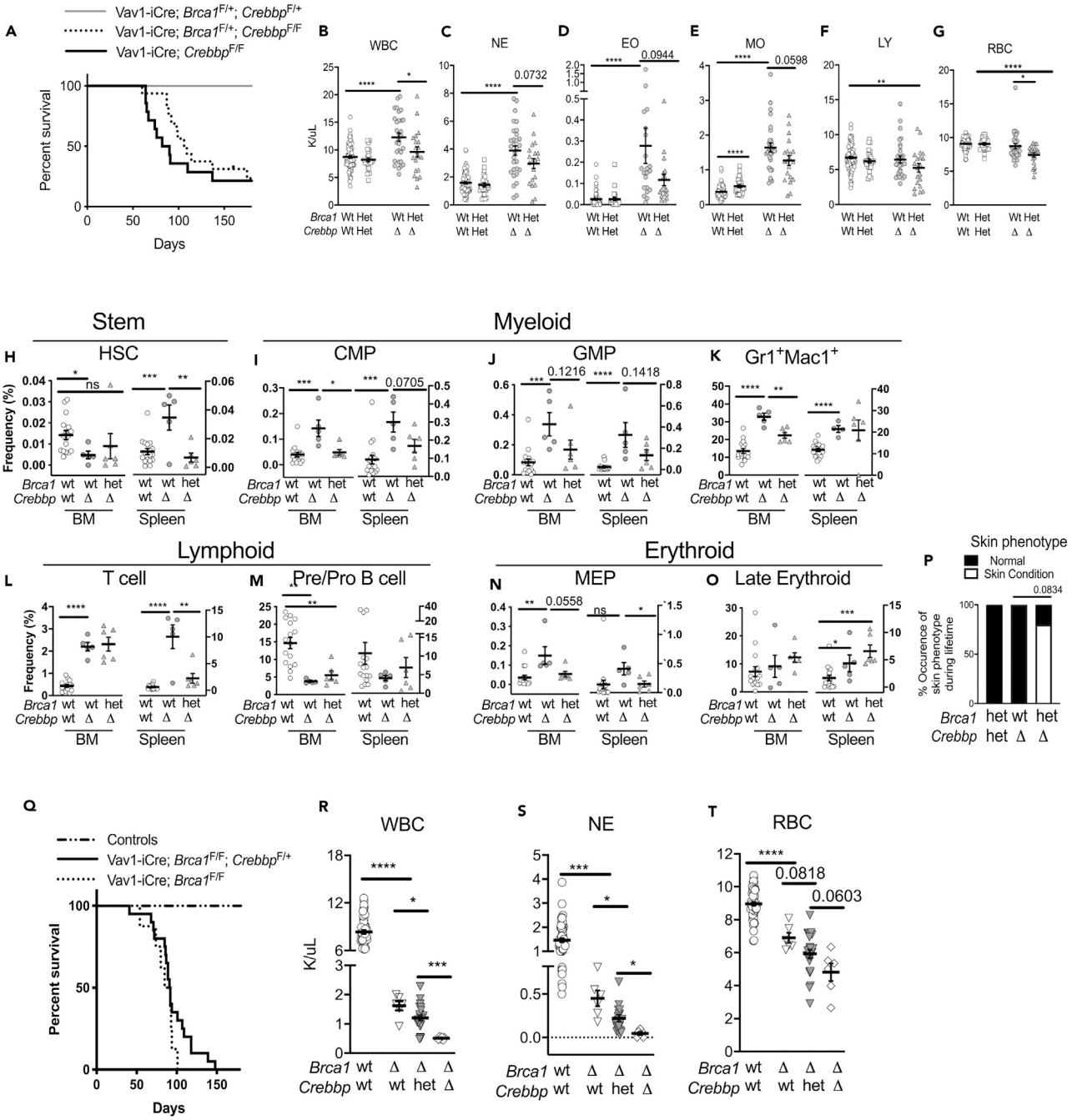

Figure 4. Heterozygosity of *Brca1* and *Crebbp* Has Hematopoietic Effects when There Is Complete Deficiency of the Other

(A–Q) *Brca1* heterozygosity in *Crebbp*-deficient bone marrow (A) results in slight, but insignificant increase in survival (Kaplan Meier, p = 0.069), attenuates elevated peripheral (B) white blood cells (WBC), (C) neutrophils (NE), (D) eosinophils (EO), (E) monocytes (MO), and (G) red blood cells (RBC), but not (F) lymphocytes (LY), (H–O) normalizes splenic HSCs, attenuates elevated myeloid progenitors in bone marrow and spleen as well as late T cell progenitors in spleen, and (P) results in slight but insignificant decreased incidence of inflammatory skin disorder (filled versus clear bars). *Crebbp* heterozygosity (Q) does not alter Brca1-deficiency survival.

(R–T) Progressive loss of *Crebbp* alleles in Brca1-deficient bone marrow results in intermediate decreases in WBCs, NE, and RBCs. Survival curve numbers: Vav1-iCre; $Brca1^{F/+}$;$Crebbp^{F/+}$ n = 12, Vav1-iCre;$Crebbp^{F/F}$ n = 14, Vav1-iCre; $Brca1^{F/+}$;$Crebbp^{F/F}$ n = 15, Vav1-iCre negative control n = 9, Vav1-iCre; $Brca1^{F/F}$ n = 8, Vav1-iCre; $Brca1^{F/F}$;$Crebbp^{F/+}$ n = 20. Blood count numbers: Vav1-iCre negative control (WT) n = 92, Vav1-iCre; $Brca1^{F/+}$;$Crebbp^{F/+}$ n = 26, Vav1-iCre;$Crebbp^{F/F}$ n = 30, Vav1-iCre; $Brca1^{F/+}$;$Crebbp^{F/F}$ n = 20. Progenitor mouse numbers: Vav1-iCre negative control n = 17, Vav1-iCre;$Crebbp^{F/F}$ n = 5,

Figure 4. *Continued*

Vav1-iCre; *Brca1*$^{F/+}$;*Crebbp*$^{F/F}$ n = 6. Skin assessment numbers: Control mice (Vav1-iCre negative) n = 32, Vav1-iCre;*Crebbp*$^{F/F}$ n = 18, Vav1-iCre; *Brca1*$^{F/+}$;*Crebbp*$^{F/F}$ n = 15.

Values represent means ± SEM. Statistical significance was assessed using a two-tailed Student's t test except in (A) where a long-rank test was used and (P) where an Fisher's exact test was used (*p < 0.05, **p < 0.01, ***p < 0.001, ****p < 0.0001).

signal for *Brca1* (Gowen et al., 1996) and (2) it is a less heterogeneous, T cell-restricted tissue compared with bone marrow and spleen.

Consistent with the prior report of transcriptional regulation of BRCA1 by CREBBP (Ogiwara and Kohno, 2012), *Brca1* mRNA in the thymus of Vav-Cre;*Crebbp*$^{F/F}$ mice (Figure 5A) was lower compared with WT BRCA1. Similarly, we found that Vav-Cre;*Crebbp*$^{F/F}$ BRCA1 protein in thymus was decreased, but to a greater extent than mRNA (Figures 5C and 5D). The specific reactivity of the mouse BRCA1 antibody (Santa Cruz SC287.17) was established in WT thymus using fully humanized BRCA1 mouse thymus as a negative control (Figure S3). Compared to WT, *Crebbp* deficiency in thymic tissue from Vav1-iCre;*Crebbp*$^{F/F}$ mice was confirmed by loss of mRNA (Figure 5B) and protein (Figure 5E). To evaluate heterogeneity of cell types in the thymus, we performed flow cytometry on *Crebbp*-deficient thymic tissue. The data were consistent with prior reports (Kasper et al., 2006; Xu et al., 2006) where Vav1-iCre;*Crebbp*$^{F/F}$ tissue showed a significant decrease in CD4+/CD8+ double-positive cell frequencies with a shift toward a higher frequency of CD4-/CD8- double-negative and CD8+ single-positive cells compared with WT (Figure S4). Because *Brca1* expression may vary between CD4 and CD8 double-positive, single-positive, and double-negative T cells, it remains possible that differences in BRCA1 protein detected between WT and Vav1-iCre;-*Crebbp*$^{F/F}$ thymus arose from changes in T cell lineages with differing levels of BRCA1.

To address issues of cell-type heterogeneity present in intact hematopoietic tissue, we also compared *Brca1* expression in primary bone marrow-derived macrophages (BMDMs) from WT and Vav1-iCre; *Crebbp*$^{F/F}$ mice. qPCR showed that WT and Vav1-iCre;*Crebbp*$^{F/F}$ differentiated BMDM cultures had similar expression levels of macrophage and dendritic cell markers F4/80 and CD11c, respectively, and suggests relative homogeneity between these two genotypes (Figures S5A and S5B, respectively). *Brca1* mRNA was not significantly different in the knockout and WT BMDMs (Figure 5F), whereas BRCA1 protein from *Crebbp*-deficient BMDMs was lower than in controls (Figures 5H and 5I). Compared to WT, *Crebbp* deficiency in BMDMs from Vav1-iCre;*Crebbp*$^{F/F}$ mice was confirmed by loss of mRNA (Figure 5G) and protein (Figure 5J). To address whether reduced levels of BRCA1 in *Crebbp*-deficient BMDMs were indirectly associated with altered proliferation rates compared with WT, we performed propidium iodide stain cell cycle analysis and found both genotypes to have similar fraction of cells in G1, G2, and S phase (Figure S5C). This is the first report of BRCA1 detection in macrophages and suggests that BRCA1 protein changes in *Crebbp*-deficient BMDMs are independent of proliferation rates and that CREBBP regulates BRCA1 using a post-transcriptional mechanism in BMDMs.

DISCUSSION

We show that mice deficient of *Crebbp* in the bone marrow present with a previously undescribed lethal systemic immune disorder that manifests as a fully penetrant, severe dermatitis and alopecia. This is consistent with a previous study that showed that a T-reg-specific double knockout of *Crebbp* and its paralog, p300, results in an early-onset lethal autoimmune disease that includes dermatitis (Liu et al., 2014). In the latter study, absence of *Crebbp* alone in T-reg cells did not result in severe autoimmunity, which suggests that systemic inflammatory disease in the Vav1-iCre;*Crebbp*$^{F/F}$ mice herein involves *Crebbp* deficiency in a broader set of immune cell types. It is clear from our studies, as well as earlier reports (Kasper et al., 2006), that *Crebbp* deficiency disrupts T cell homeostasis beyond T-reg function as shown with increase in CD8 single-positive cells in thymus. Whether this translates to elevation in CD8-positive autoreactive and effector T-cells to mediate full-blown skin disease needs further investigation. A role for neutrophils in autoimmune disease has been reported (Nemeth and Mocsai, 2012). Therefore, presence of granulocytes in the dermal layers prior to skin abnormalities may potentiate later phases of autoimmune processes. Finally, it is also possible that *Crebbp*-deficient mice display impaired wound healing responses in the event that hematopoietic loss of *Crebbp* disrupts M2 macrophages differentiation or function.

Crebbp deficiency also led to a much earlier and more severe myeloproliferative phenotype compared with previous reports in older haploinsufficient mice (Kung et al., 2000; Rebel et al., 2002; Zhou et al., 2016; Zimmer et al., 2012). This further confirms the importance of *Crebbp* in hematopoiesis and

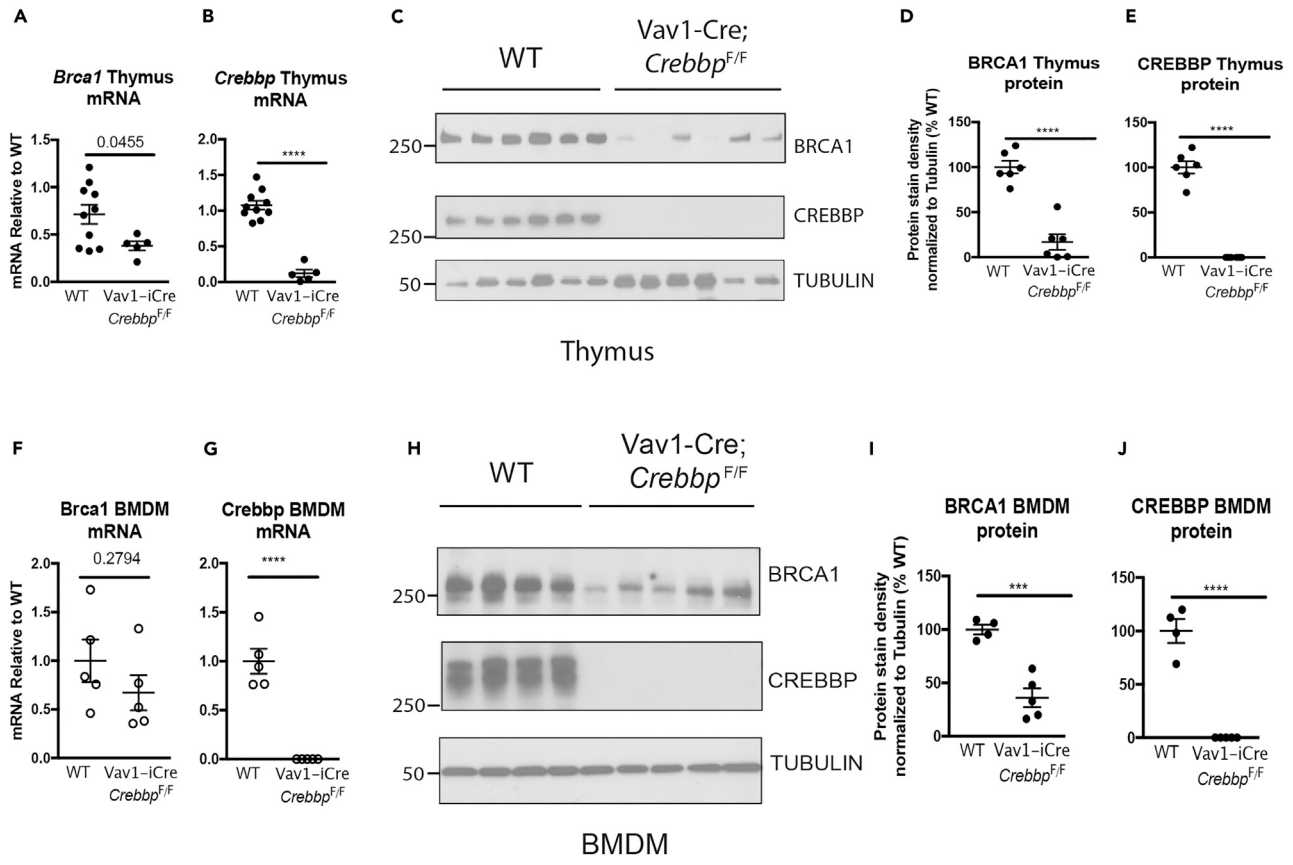

Figure 5. Decreased BRCA1 Protein Levels in CREBBP-Deficient Tissue

(A–C) *Crebbp*-deficient thymus has decreased levels of (A) *Brca1* mRNA and (C) BRCA1 protein. *Crebbp*-deficiency in Vav1-iCre; $Crebbp^{F/F}$ thymus was verified by (B) qPCR and (C) western blot.

(D) and (E) show densitometry of western blot signal in thymus.

(F–H) (F) BMDMs harvested after 6 days of culture in granulocyte-macrophage colony stimulating factor (GM-CSF) (20 ng/mL) from *Crebbp*-deficient bone marrow-derived macrophages (BMDMs) show similar *Brca1* mRNA in all genotypes but (H) lower BRCA1 protein. *Crebbp* deficiency in Vav1-iCre;$Crebbp^{F/F}$ BMDMs was verified by (G) qPCR and (H) western blot.

(I) and (J) show densitometric analysis of BMDM western blot data. Thymus *Brca1* mRNA was measured in WT (n = 10) and Vav1-iCre; $Crebbp^{F/F}$(n = 5) mice. Thymic BRCA1 protein was measured in WT (n = 6) and Vav1-iCre; $Crebbp^{F/F}$(n = 6) mice. BMDM *Brca1* mRNA was measured in WT (n = 5) and Vav1-iCre; $Crebbp^{F/F}$(n = 5) mice. BMDM BRCA1 protein was measured in WT (n = 4) and Vav1-iCre;$Crebbp^{F/F}$ mice (n = 5).

Values represent means ± SEM. Statistical significance was assessed using a two-tailed Student's t test (***p < 0.001, ****p < 0.0001).

supports earlier studies that show that *Crebbp* acts as a key immune modulator of inflammatory cell activity and differentiation in the bone marrow (Chan et al., 2011; Lennard Richard et al., 2016; Liu et al., 2013, 2014). Our data suggest that loss of *Crebbp* results in HSC mobilization, evidenced by HSC population balance shifting from bone marrow to spleen, as well as a consistent granulocytosis. The neutrophilia and monocytosis was a fully penetrant phenotype present before full-blown skin disease, suggesting that leukocytosis in *Crebbp*-deficient mice is an inherent, rather than acquired (e.g., infection), condition. Therefore, it is attractive to speculate that *Crebbp* is required to prevent inappropriate HSC mobilization and that modulating *Crebbp* may be a mechanism to regulate hematopoiesis and innate immune responses.

The abundance of splenic HSCs in our *Crebbp*-deficient mice show that *Crebbp* is not required to maintain an adequate pool of HSCs per se. This differs from previous reports that *Crebbp* displays cell autonomous and non-autonomous haploinsufficiency in bone marrow to maintain functional self-renewing HSCs (Rebel et al., 2002; Zimmer et al., 2011). These conclusions were based on reduced secondary transplant efficiency associated with lower LSK CD34-populations in the bone marrow of *Crebbp* heterozygous mice. Similarly, a later study showed that deletion of *Crebbp* in adult HSC also resulted in a lower reconstitution capacity as

well as decreased frequency of LSK CD34$^-$Flt3$^-$ cells that was independent of mobilization to the spleen (Chan et al., 2011). A possible reason for the discrepancy between our and earlier splenic HSC quantification is that we confine our estimation to the LSK CD150$^+$CD48$^-$ (Kiel et al., 2005) population that is more enriched for self-renewing HSCs, rather than multipotent and early progenitors, used in earlier studies. Owing to the mixed background of our mice in this study, we were unable to address the transplant repopulation capacity of *Crebbp*-deficient HSCs.

We show that co-deletion of tumor suppressors *Crebbp* and *Brca1* in bone marrow results in shortened lifespan compared with the already reduced survival of single knockouts. The advanced pancytopenia in DKOs highlights an ability of *Crebbp* to compensate for *Brca1* at an early stage of hematopoiesis. BRCA1 deficiency in cells is often associated with DNA damage-induced apoptosis that arises from defects in multiple pathways of DNA repair, including nuclear excision repair (Hartman and Ford, 2002), transcription-coupled repair of oxidative DNA damage (Abbott et al., 1999), homologous recombinational repair (Moynahan et al., 1999; Snouwaert et al., 1999), and non-homologous end-joining (Baldeyron et al., 2002; Zhong et al., 2002a, 2002b). Since *Crebbp* has recently been shown to maintain genomic integrity during lineage specification of hematopoietic cells (Horton et al., 2017), CREBBP may partially compensate for defective DNA repair in *Brca1*-deficient HSCs and progenitors. We hypothesize that combined deletion of *Brca1* and *Crebbp* results in more severe global DNA damage than with *Brca1* and *Crebbp* single knockouts and that accelerated accumulation of genomic abnormalities leads to accelerated cell death rather than transformation. We therefore hypothesize that complete inhibition or loss of both tumor suppressors in blood cancers may be synthetic lethal, and if it is, this concept could be exploited to develop therapeutic targets of each in either *Brca1*- or *Crebbp*-deficient cancers.

Finally, we show that BRCA1 protein is altered in *Crebbp*-deficient hematopoietic tissue. In thymus, decreased BRCA1 protein in *Crebbp*-deficient thymus correlates with decreased *Brca1* mRNA, which is consistent with prior reports that *Brca1* is under transcriptional regulation by *Crebbp* (Ogiwara and Kohno, 2012). In contrast, *Crebbp*-deficient BMDMs have decreased BRCA1 protein with no significant decrease in *Brca1* mRNA, suggesting the possibility of post-transcriptional regulation of BRCA1 protein by CREBBP. Although our data show that BRCA1 levels are decreased in CREBBP-deficient hematopoietic tissue, our *in vivo* data do not support a simplistic hypothesis that *Crebbp*-deficient phenotypes arise owing to loss of BRCA1 protein. It is interesting to speculate that reduced leukocytosis with *Brca1* heterozygosity in *Crebbp*-deficient mice (Figures 4B–4D) may reflect a reduction of BRCA1 protein below haploinsufficient levels that occurs in WT mice.

The compensatory roles for *Brca1* and *Crebbp* will lead us to further investigate how these tumor suppressor genes cooperate in developmental systems and how heterozygosity of pathogenic mutations in each gene contributes to tumorigenesis that results from the loss of the other.

Limitations of the Study

Key limitations of this study relate to the poor health of *Crebbp/Brca1* DKO mice. The number of surviving DKO mice was low, and this limited statistical power for more in depth *in vivo* analyses. For example, since hematopoietic tissue was depleted we could not expand primary cells in culture or perform extensive biochemical analyses. Inducible systems will circumvent early lethality and allow for the comparison of the acute effects of co-deleting both genes *in vivo* as well as in culture. Another significant limitation was our inability to assess HSC self-renewal capacities with transplantation experiments as the Crebbp allele was obtained from a mixed background.

METHODS

All methods can be found in the accompanying Transparent Methods supplemental file.

SUPPLEMENTAL INFORMATION

Supplemental Information can be found online at https://doi.org/10.1016/j.isci.2019.08.031.

ACKNOWLEDGMENTS

We thank members of the Ross lab for their intellectual contributions to this work. This work was supported by NIH R01 HL132251-02, the Nancy Tartaglino Richards Cancer Genetics Research Fund, the Lucy and

Henry Billingsley Fund and a Burroughs Wellcome Fund Clinical Scientist Award in Translational Research (TSR). TSR holds the Jeanne Ann Plitt Professorship in Breast Cancer Research and the H. Ben and Isabelle T. Decherd Chair in Internal Medicine at UT Southwestern Medical Center.

AUTHOR CONTRIBUTIONS

T.S.R., S.R.H., R.W., and V.E.M. conceived the study and designed/interpreted the experiments. S.R.H. and T.S.R. wrote the manuscript. S.R.H., R.W., K.M., and V.E.M. performed experiments and collected the data.

DECLARATION OF INTERESTS

The authors declare no competing interests.

Received: October 4, 2018
Revised: January 13, 2019
Accepted: August 19, 2019
Published: September 27, 2019

REFERENCES

Abbott, D.W., Thompson, M.E., Robinson-Benion, C., Tomlinson, G., Jensen, R.A., and Holt, J.T. (1999). BRCA1 expression restores radiation resistance in BRCA1-defective cancer cells through enhancement of transcription-coupled DNA repair. J. Biol. Chem. *274*, 18808–18812.

Akashi, K., Traver, D., Miyamoto, T., and Weissman, I.L. (2000). A clonogenic common myeloid progenitor that gives rise to all myeloid lineages. Nature *404*, 193–197.

Baldeyron, C., Jacquemin, E., Smith, J., Jacquemont, C., De Oliveira, I., Gad, S., Feunteun, J., Stoppa-Lyonnet, D., and Papadopoulo, D. (2002). A single mutated BRCA1 allele leads to impaired fidelity of double strand break end-joining. Oncogene *21*, 1401–1410.

Chan, W.I., Hannah, R.L., Dawson, M.A., Pridans, C., Foster, D., Joshi, A., Gottgens, B., Van Deursen, J.M., and Huntly, B.J. (2011). The transcriptional coactivator Cbp regulates self-renewal and differentiation in adult hematopoietic stem cells. Mol. Cell. Biol. *31*, 5046–5060.

Futreal, P.A., Liu, Q., Shattuck-Eidens, D., Cochran, C., Harshman, K., Tavtigian, S., Bennett, L.M., Haugen-Strano, A., Swensen, J., Miki, Y., et al. (1994). BRCA1 mutations in primary breast and ovarian carcinomas. Science *266*, 120–122.

Georgiades, P., Ogilvy, S., Duval, H., Licence, D.R., Charnock-Jones, D.S., Smith, S.K., and Print, C.G. (2002). VavCre transgenic mice: a tool for mutagenesis in hematopoietic and endothelial lineages. Genesis *34*, 251–256.

Gowen, L.C., Johnson, B.L., Latour, A.M., Sulik, K.K., and Koller, B.H. (1996). Brca1 deficiency results in early embryonic lethality characterized by neuroepithelial abnormalities. Nat. Genet. *12*, 191–194.

Hartman, A.R., and Ford, J.M. (2002). BRCA1 induces DNA damage recognition factors and enhances nucleotide excision repair. Nat. Genet. *32*, 180–184.

Horton, S.J., Giotopoulos, G., Yun, H., Vohra, S., Sheppard, O., Bashford-Rogers, R., Rashid, M., Clipson, A., Chan, W.I., Sasca, D., et al. (2017). Early loss of Crebbp confers malignant stem cell properties on lymphoid progenitors. Nat. Cell Biol. *19*, 1093–1104.

Kasper, L.H., Fukuyama, T., Biesen, M.A., Boussouar, F., Tong, C., de Pauw, A., Murray, P.J., van Deursen, J.M., and Brindle, P.K. (2006). Conditional knockout mice reveal distinct functions for the global transcriptional coactivators CBP and p300 in T-cell development. Mol. Cell. Biol. *26*, 789–809.

Kiel, M.J., Yilmaz, O.H., Iwashita, T., Yilmaz, O.H., Terhorst, C., and Morrison, S.J. (2005). SLAM family receptors distinguish hematopoietic stem and progenitor cells and reveal endothelial niches for stem cells. Cell *121*, 1109–1121.

Kung, A.L., Rebel, V.I., Bronson, R.T., Ch'ng, L.E., Sieff, C.A., Livingston, D.M., and Yao, T.P. (2000). Gene dose-dependent control of hematopoiesis and hematologic tumor suppression by CBP. Genes Dev. *14*, 272–277.

Lennard Richard, M.L., Brandon, D., Lou, N., Sato, S., Caldwell, T., Nowling, T.K., Gilkeson, G., and Zhang, X.K. (2016). Acetylation impacts Fli-1-driven regulation of granulocyte colony stimulating factor. Eur. J. Immunol. *46*, 2322–2332.

Liu, Y., Wang, L., Predina, J., Han, R., Beier, U.H., Wang, L.C., Kapoor, V., Bhatti, T.R., Akimova, T., Singhal, S., et al. (2013). Inhibition of p300 impairs Foxp3(+) T regulatory cell function and promotes antitumor immunity. Nat. Med. *19*, 1173–1177.

Liu, Y., Wang, L., Han, R., Beier, U.H., Akimova, T., Bhatti, T., Xiao, H., Cole, P.A., Brindle, P.K., and Hancock, W.W. (2014). Two histone/protein acetyltransferases, CBP and p300, are indispensable for Foxp3+ T-regulatory cell development and function. Mol. Cell. Biol. *34*, 3993–4007.

Mgbemena, V.E., Signer, R.A., Wijayatunge, R., Laxson, T., Morrison, S.J., and Ross, T.S. (2017). Distinct Brca1 mutations differentially reduce hematopoietic stem cell function. Cell Rep. *18*, 947–960.

Miki, Y., Swensen, J., Shattuck-Eidens, D., Futreal, P.A., Harshman, K., Tavtigian, S., Liu, Q., Cochran, C., Bennett, L.M., Ding, W., et al. (1994). A strong candidate for the breast and ovarian cancer susceptibility gene BRCA1. Science *266*, 66–71.

Miller, R.W., and Rubinstein, J.H. (1995). Tumors in Rubinstein-Taybi syndrome. Am. J. Med. Genet. *56*, 112–115.

Moynahan, M.E., Chiu, J.W., Koller, B.H., and Jasin, M. (1999). Brca1 controls homology-directed DNA repair. Mol. Cell *4*, 511–518.

Nemeth, T., and Mocsai, A. (2012). The role of neutrophils in autoimmune diseases. Immunol. Lett. *143*, 9–19.

Ogiwara, H., and Kohno, T. (2012). CBP and p300 histone acetyltransferases contribute to homologous recombination by transcriptionally activating the BRCA1 and RAD51 genes. PLoS One *7*, e52810.

Pao, G.M., Janknecht, R., Ruffner, H., Hunter, T., and Verma, I.M. (2000). CBP/p300 interact with and function as transcriptional coactivators of BRCA1. Proc. Natl. Acad. Sci. U S A *97*, 1020–1025.

Rebel, V.I., Kung, A.L., Tanner, E.A., Yang, H., Bronson, R.T., and Livingston, D.M. (2002). Distinct roles for CREB-binding protein and p300 in hematopoietic stem cell self-renewal. Proc. Natl. Acad. Sci. U S A *99*, 14789–14794.

Schorry, E.K., Keddache, M., Lanphear, N., Rubinstein, J.H., Srodulski, S., Fletcher, D., Blough-Pfau, R.I., and Grabowski, G.A. (2008). Genotype-phenotype correlations in Rubinstein-Taybi syndrome. Am. J. Med. Genet. A *146A*, 2512–2519.

Snouwaert, J.N., Gowen, L.C., Latour, A.M., Mohn, A.R., Xiao, A., DiBiase, L., and Koller, B.H. (1999). BRCA1 deficient embryonic stem cells display a decreased homologous recombination frequency and an increased frequency of non-homologous recombination that is corrected by expression of a brca1 transgene. Oncogene *18*, 7900–7907.

Vasanthakumar, A., Arnovitz, S., Marquez, R., Lepore, J., Rafidi, G., Asom, A., Weatherly, M., Davis, E.M., Neistadt, B., Duszynski, R., et al. (2016). Brca1 deficiency causes bone

marrow failure and spontaneous hematologic malignancies in mice. Blood *127*, 310–313.

Xu, W., Fukuyama, T., Ney, P.A., Wang, D., Rehg, J., Boyd, K., van Deursen, J.M., and Brindle, P.K. (2006). Global transcriptional coactivators CREB-binding protein and p300 are highly essential collectively but not individually in peripheral B cells. Blood *107*, 4407–4416.

Zhong, Q., Boyer, T.G., Chen, P.L., and Lee, W.H. (2002a). Deficient nonhomologous end-joining activity in cell-free extracts from Brca1-null fibroblasts. Cancer Res. *62*, 3966–3970.

Zhong, Q., Chen, C.F., Chen, P.L., and Lee, W.H. (2002b). BRCA1 facilitates microhomology-mediated end joining of DNA double strand breaks. J. Biol. Chem. *277*, 28641–28647.

Zhou, T., Perez, S.N., Cheng, Z., Kinney, M.C., Lemieux, M.E., Scott, L.M., and Rebel, V.I. (2016). Context matters: distinct disease outcomes as a result of crebbp hemizygosity in different mouse bone marrow compartments. PLoS One *11*, e0158649.

Zimmer, S.N., Zhou, Q., Zhou, T., Cheng, Z., Abboud-Werner, S.L., Horn, D., Lecocke, M., White, R., Krivtsov, A.V., Armstrong, S.A., et al. (2011). Crebbp haploinsufficiency in mice alters the bone marrow microenvironment, leading to loss of stem cells and excessive myelopoiesis. Blood *118*, 69–79.

Zimmer, S.N., Lemieux, M.E., Karia, B.P., Day, C., Zhou, T., Zhou, Q., Kung, A.L., Suresh, U., Chen, Y., Kinney, M.C., et al. (2012). Mice heterozygous for CREB binding protein are hypersensitive to gamma-radiation and invariably develop myelodysplastic/myeloproliferative neoplasm. Exp. Hematol. *40*, 295–306.e5.

ISCI, Volume *19*

Supplemental Information

Functional Interaction of BRCA1 and CREBBP in Murine Hematopoiesis

Sam R. Holmstrom, Ranjula Wijayatunge, Kelly McCrum, Victoria E. Mgbemena, and Theodora S. Ross

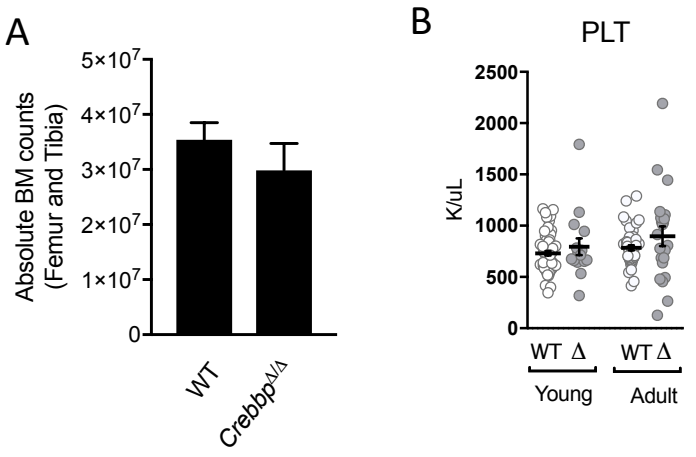

Figure S1. *Crebpp* deficiency in bone marrow does not result in thrombocytopenia (Related Figure

A) No difference in bone marrow cellularity between control (WT) and $^{F/F}$ mice. **B)** Platelets were not different between WT (Vav1-iCre negative, open circles) and Vav1-iCre;*Crebbp*$^{F/F}$ mice (grey circles) at young (4-8 weeks) or adult (>8-24 weeks) age. Numbers are the same as in Figure 2 for other CBC parameters. Values represent mean ±SEM. Statistical significance was assessed using a two-tailed Student's t test (*p<0.05, **p<0.01, ***p<0.001, ****p<0.0001).

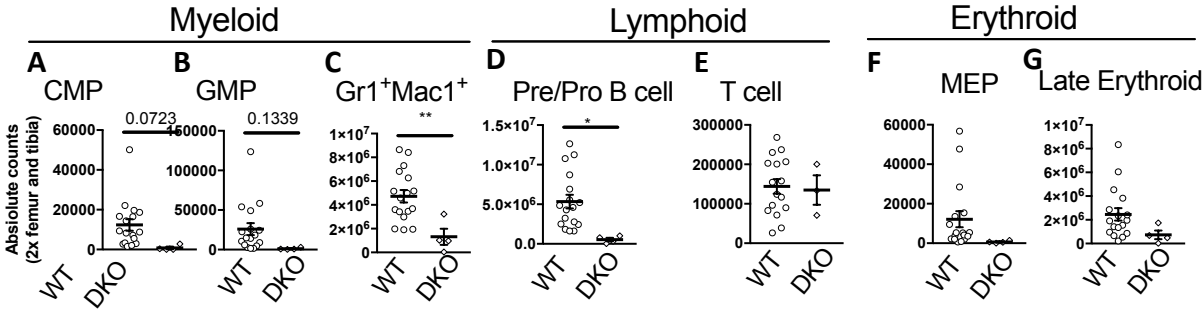

Figure S2. *Crebbp/Brca1* DKO mice have decreased absolute bone marrow progenitor counts. **A-G)** Flow cytometric analysis of **A)** CMP, **B)** GMP, **C)** GM, **D)** B-cell progenitor, **E)** T-cell progenitor, **F)** MEP, and **G)** erythroid progenitor absolute counts from 4-8 week old Vav1-iCre *Brca1*$^{F/F}$;*Crebbp*$^{F/F}$ DKOs (n=4) compared to age-matched littermate controls (n=15). Values represent mean ±SEM. Statistical significance was assessed using a two-tailed Student's t test (*p<0.05, **p<0.01, ***p<0.001, ****p<0.0001).

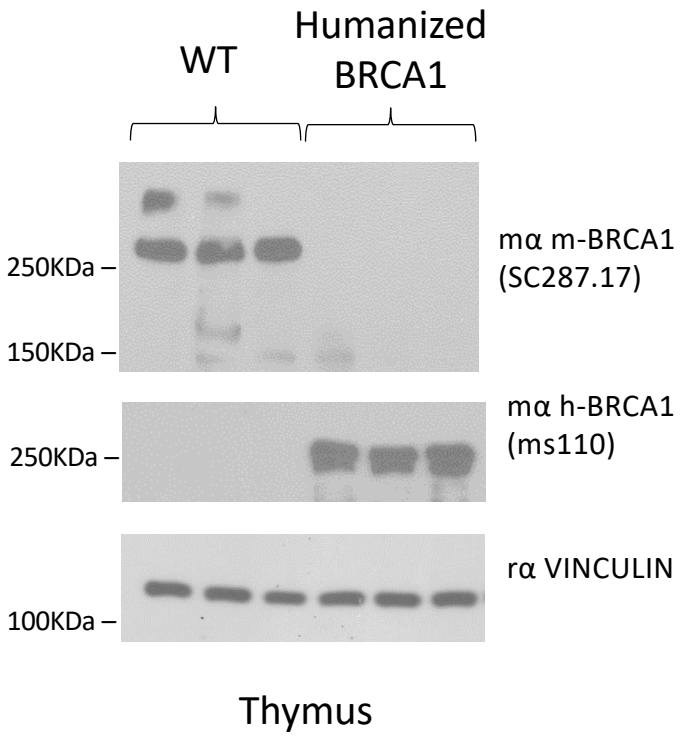

Figure S3. Validation of BRCA1 protein signal in mouse tissue. Specificity of BRCA1 western blot signal with mouse reactive anti-BRCA1 Santa Cruz antibody SC287-17 was verified using a humanized *BRCA1* mouse model as a negative control. Conversely, presence of BRCA1 in thymus of humanized BRCA1 mice was detected with human reactive MS110.

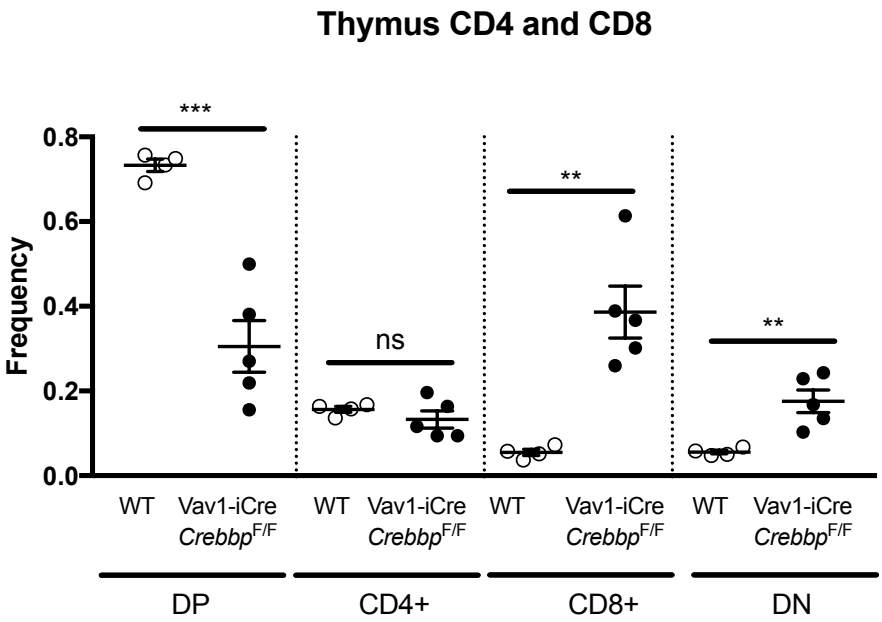

Figure S4. Flow cytometric analysis of *Crebbp*-deficient thymus shows abnormal T-cell lineage frequencies. Population frequencies of CD4 and CD8 double positive, single positive and double negative cells in thymus of WT and Vav1-iCre; *Crebbp*$^{F/F}$ mice was compared using flow cytometry. Values represent mean ±SEM. Statistical significance was assessed using a two-tailed Student's t test (*p<0.05, **p<0.01, ***p<0.001, ****p<0.0001) (n=5 for each genotype).

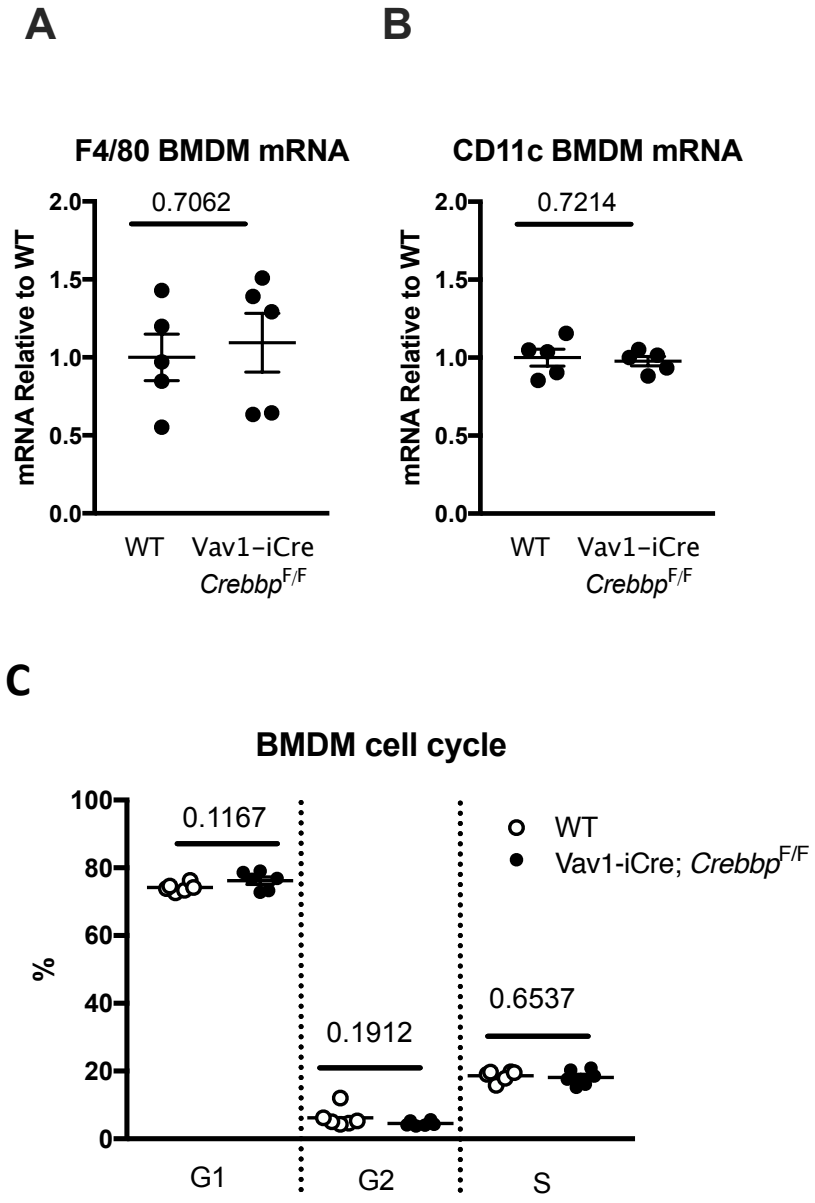

Figure S5. Evaluation of cell type purity in WT and Crebbp-deficient bone marrow derived macrophages (BMDMs). Mature BMDMs from WT and *Crebbp*-deficient mice harvested after 6 days of culture in GM-CSF (20ng/ml) showed similar variation in real time QPCR detection of **A)** dendritic cell (CD11c) and **B)** macrophage-specific (F4/80) markers in both WT and Vav1-iCre; *Crebbp*$^{F/F}$. **C)** Propridium iodide stain and flow cytometric analysis of cell cycle of matured BMDMs from WT and Vav1-iCre;*Crebbp*$^{F/F}$ mice showed similar fraction of cells in G_1, G_2 and S phases. Values represent mean ±SEM. Statistical significance was assessed using a two-tailed Student's t test (*p<0.05, **p<0.01, ***p<0.001, ****p<0.0001), (n=4-5).

Table S1. *Crebbp* deficiency phenotype summary (related to Figure 2)-page 1/3

Pheno-type	germline or cre driver	*Crebbp* allele		Previous studies	Current study: Vav1-iCre;*Crebbp*$^{F/F}$, 4-8 weeks of age (unless otherwise noted)
HSCs	germline	Heterozygous deletion	(Rebel et al., 2002)	*Crebbp* is necessary for HSC self-renewal. Number of functional HSCs (LSK CD34-) was lower in >9 months mice and have reduced self-renewal capacity during serial transplantation.	*Crebbp* is not required to maintain an adequate pool of HSCs per se. Reduced BM HSC frequencies (CD150+CD48-Lineage-Sca-1+ckit+;CD150+CD48-LSK) was seen in 4-8 week old mice, with increased SP HSC frequencies suggesting HSC mobilization or extramedullary hematopoiesis (EMH). The discrepancy with previous reports may be because this HSC population is highly enriched for self-renewing HSCs, rather than multipotent and early progenitors (Kiel et al., 2005). Due to the mixed background of our mice in this study, we were unable to address the transplant repopulation capacity of *Crebbp*-deficient HSCs.
	germline	Heterozygous deletion	(Zimmer et al., 2012)	*Crebbp*+/ 9-12 old mice showed decreased long-term HSCs (LSK CD34-).	
	MX1-cre	biallelic deletion	(Chan et al., 2011)	Ablation of *Crebbp* in hematopoietic tissues of adult mice reduced BM HSC (LSK CD34-Flt3-) frequencies, with no change in spleen HSC frequencies. Reduction of HSC-enriched population led to exhaustion of HSCs upon serial transplantation and replicative stress.	
Myeloproliferation	germline	Heterozygous deletion	(Kung et al., 2000)	*Crebbp* is important for maintaining normal levels of early progenitors of the myeloid lineage. Increased myeloid (Mac1+Gr+) and erythroid (TER119+) progenitors in the spleen in old (>12 months) mice with splenomegaly. These mice also showed decreased BM cellularity and modest but significant decreases in BM hematopoietic cell types and significant increase in myeloid cells in PB. No changes in BM cellularity observed at 8 weeks of age.	Ablation of *Crebbp* leads to myeloproliferation. By 4-8 weeks of age, Vav1-iCre;*Crebbp*$^{F/F}$ mice show increased myeloid progenitors (CMP, GMP, gran/mono late) in both BM and SP. Also, increased MEPs in BM and SP. Increased late erythroid progenitors in BM. Leukocytosis seen at 4-8 weeks of age with increased WBCs (NE, MO, EO) in PB. However, lymphocyte counts were normal.
	germline	Heterozygous deletion	(Zimmer et al., 2011)	*Crebbp* is necessary for maintaining the normal BM microenvironment, and it's deficiency leads to myeloproliferation. Five months after transplantation, irradiated *Crebbp*+/- mice transplanted with WT BM show increased myelopoeisis (increased myeloid cells in BM). They already saw increased myeloid cells in PB, 8 weeks after transplantation.	
	MX1-cre	biallelic deletion	(Chan et al., 2011)	Peripheral myeloid cells trended to increase at 4-weeks post pIpC treatment (6-10 week old mice were treated with pIpC for 10 days) and show a significant increase at 28 weeks. Increase in myelpoid progenitor to LSK CD34-Flt3- ratio.	

Table S1. *Crebbp* deficiency phenotype summary (related to Figure 2)- page 2/3

Pheno-type	germline or cre driver	*Crebbp* allele		Previous studies	Current study: Vav1-iCre;*Crebbp*$^{F/F}$, 4-8 weeks of age (unless otherwise noted)
Lymphocytes/Thymus	CD19-cre	biallelic deletion	(Xu et al., 2006)	Impaired B-cell maturation. Loss of *Crebbp* at Pro-B cell stage lead to moderate decreases in B-cell number in PB and SP, with no changes in T-cell number. Although no significant alteration in ProB and PreB ratios were seen in BM, there was a decrease in mature B cells.	No change in lymphocyte counts in PB. Increased CD3+ T-cell progenitors in BM and SP. Reduced ProB/PreB-cell frequencies (CD43-B220hi/B220lo) in BM with less of an effect in spleen. In thymus significant decrease in CD4+/CD8+ double positive cell frequencies with a shift toward a higher frequency of CD4-/CD8- double negative and CD8+ single positive cells compared to WT.
	germline	Heterozygous deletion	(Zimmer et al., 2011)	Impaired B-cell maturation. When WT BM were transplanted into lethally irradiated *Crebbp*+/- mice, the frequency of BM B-cells (B220+) was found to be decreased 5 months after transplantation.	
	Lck-Cre	biallelic deletion	(Kasper et al., 2006)	Deletion of *Crebbp* in CD4-/CD8- double negative thymocytes leads to defective B- and T-cell development in adult mice, specifically a decrease in CD4+/CD8+ double positive thymocytes and an increase in CD8+ single positive thymocytes.	
	germline	Heterozygous deletion	(Kung et al., 2000)	Reduced B cell counts in PB and modest but significant decrease in colony forming capacity of pre-B and myeloid progenitors. Reduced B and T progenitors in BM. Some B and T cell abnormalities were apparent by 3 months of age.	
Inflammatory disorder	Foxp3-cre	biallelic deletion	(Liu et al., 2014)	Double knockout of *Crebbp* and its paralog *p300* in T-reg cells results in an early-onset lethal autoimmune disease that includes dermatitis. Absence of *Crebbp* alone in T-reg cells did not result in autoimmunity.	Lethal systemic immune disorder and associated severe dermatitis and alopecia seen by 4-5 weeks of age.

Table S1. *Crebbp* deficiency phenotype summary (related to Figure 2)- page 3/3

Pheno-type	germline or cre driver	*Crebbp* allele		Previous studies	Current study: Vav1-iCre;*Crebbp*$^{F/F}$, 4-8 weeks of age (unless otherwise noted)
Hematopoietic malignancies	germline	Heterozygous deletion	(Kung et al., 2000)	Hematologic neoplasias with advanced age; of *Crebbp*+/- mice between 10 and 21 months of age, 39% either developed hematologic neoplasia with leukemia and tumors of hematopoietic origin or harbored tumorigenic cells.	Due to the sever skin phenotype, Vav1-iCre;*Crebbp*$^{F/F}$ mice had to be terminated at a young age (median survival 86 days). Neither Vav1-iCre;*Crebbp*$^{F/F}$ nor Vav1-iCre;*Crebbp*$^{F/+}$ mice developed leukemias or other hematological neoplasias by 4-8 weeks of age.
	CD19-cre	biallelic deletion	(Xu et al., 2006)	Loss of *Crebbp* at Pro-B cell stage does not result in B-cell lymphomas, although there was increased death due to unknown causes after 1 year of age.	
	germline	Heterozygous deletion	(Zhou et al., 2016)	Adult *Crebbp*+/- mice or WT mice transplanted with *Crebbp*+/- BM develop myelodysplasia, acute myeloid leukemia (AML), and myelodysplastic syndrome (MDS).	
	germline	Heterozygous deletion	(Zimmer et al., 2012)	Adult *Crebbp*+/- mice (9-12 months) develop dysplastic features.	
Thrombocytopenia	MX1-cre	biallelic deletion	(Chan et al., 2011)	Thrombocytopenia was seen in adulthood.	No thrombocytopenia was seen in young (4-12 week) or adult (8-24 weeks) mice.

TRANSPARENT METHODS

Transgenic Mice. The *Brca1*$^{F22\text{-}24}$ (McCarthy et al., 2007), *Crebbp*$^{f/f}$ (Kang-Decker et al., 2004), *Vav1-iCre* (Georgiades et al., 2002) *Brca1*^{BRCA1} (Mgbemena et al., 2017) alleles have been previously described and are distributed by Jackson Labs. Mice were housed in the Unit for Laboratory Animal Medicine at the University of Texas Southwestern Medical School under specific pathogen-free conditions. All mouse experiments were conducted after approval of the UT Southwestern Medical Center Committee on the Use and Care of Animals.

Genotype analysis. Mice were genotyped from tail snips using Real-Time PCR assays designed by Transnetyx.

Histology. Mice were necropsied and tissue fixed in 4% paraformaldehyde (PFA). Sections were stained with H&E (UT Southwestern Histo Pathology Core).

Hematopoietic analysis. Complete blood cell count analysis was performed on peripheral blood using the Hemavet 950 with MULTI-TROL Mouse as an equilibration control (Drew Scientific). For flow cytometry bone marrow were isolated by flushing the long bones (femurs and tibias) in Ca^{2+} and Mg^{2+} free Hank's buffered salt solution (Corning) supplemented with 3% heat-inactivated bovine serum (Gibco). Spleens and thymus were prepared by crushing tissue. All cells were filtered through a 40-μm cell strainer to obtain single cell suspensions. Single-cell suspensions of splenocytes and bone marrow cells, but not thymus, were depleted of mature red blood cells by hypotonic lysis with ACK lysis buffer (Thermo Fisher). Cell number was determined by manual counting on a hemocytometer. Flow cytometric analysis of specific hematopoietic progenitors was performed as previously described (Foley et al., 2013; Mgbemena et al., 2017). Bone marrow and spleen cells were analyzed for lineage (CD3, B220, Mac-GR1, Ter119), progenitor (lin-,Sca-,c-kit+, CD16/32+), and HSC (lin−, Sca+, cKit+, CD48- CD150+) markers and thymus T-cell lineages were determined with CD4+ and CD8+ using the FACSCanto II RUO flow cytometer (BD). Data was analyzed using FlowJo Software. BMDM purity was determined by real time QPCR using Taqman probes (Invitrogen) for macrophage marker F4/80 and dendritic cell marker CD11c.

Cell culture and reagents. For BMDM cultures, bone marrow cells were isolated by spinning the long bones (femurs and tibias) cut at the ends at 8,000g for 2 mins. Cells were filtered through a 70-μm cell strainer to obtain single cell suspensions. Cell number was determined by manual counting on a hemocytometer. The bone marrow cells were suspended in RPMI-1640 (Gibco) containing 1% L-glutamine, 1% Pen/Strep, 20% FBS and 20 ng/mL GM-CSF (Shenandoah Biotech). Cells were plated at 0.5 x 10^6 cells per well in 6-well plates. Cells were incubated for 6 days at 37 °C and 5% CO2 with medium change on day 3.

Cell cycle analysis. For cell cycle analysis, BMDMs were trypsinized, ethanol fixed, and stained with 80 μg/mL propidium iodide (PI) (Sigma) for 20 mins at room temperature. Flow cytometry data were acquired on a FACS LSRFortessa SORP (Becton Dickinson) and were analyzed using FlowJo software.

***RNA isolation and quantitative real time PCR*.** RNA was isolated using TRIzol reagent (Invitrogen) according to manufacturer's instructions. RNA concentrations were quantified with the Nanodrop 2000 Spectrophotometer (Thermo Scientific). cDNA was generated from 1ug of total RNA using iScript Reverse Transcription Supermix (BIO RAD). Real-time PCR was run using Taqman probes (Invitrogen) in an ABI 7300 real time PCR machine (Applied Biosystems). GAPDH was used as an internal control and the ΔΔcT method was used to calculate fold changes in expression.

Total protein extraction and Western blotting. For total BMDM protein extraction, cells were rinsed once in cold 1X PBS, lysed in ice-cold lysis buffer (50mM Tris pH7.4, 250mM NaCl, 25mM EGTA, 100mM $MgCl_2$, 1%Triton X-100, 10% glycerol) with protease inhibitors (Complete tablets, Roche) for 1hr, sonicated, and cleared of insoluble components by centrifugation at 16,000g at 4° C for 30 mins. Mouse thymic tissue was prepared in RIPA lysis buffer (Cell Signaling Technology) supplemented with 50mM NaF, 0.1% SDS, 1mg/ml Pefabloc, 1mM PMSF, and protease inhibitors (Complete tablets, Roche). Tissues were homogenized in cold lysis buffer with an electric homogenizer, sonicated, and spun at 4°C.

Approximately 20-80 ug of protein was resolved by SDS-PAGE (6% or 10% Tris-glycine gels) and transferred to PVDF membrane (Perkin Elmer) using a wet electroblotting system (BIO RAD). Membranes were blocked in 5% (w/v) dry milk in PBS-Tween-20 (0.5% v/v) and probed with appropriate primary antibodies. Blots were incubated with horseradish peroxidase (HRP)-conjugated mouse or rabbit secondary antibodies (1:5,000; GE healthcare). Signals were detected using ECL (Pierce). HIP1, ACTIN, TUBULIN, or VINCULIN were used as loading controls. Western blot protein bands were quantified using ImageJ Software (NIH).

Antibodies. All antibodies were used at 1:1000 dilution unless otherwise specified. Antibodies used were: mouse monoclonal anti-ACTIN (Cell Signaling), mouse monoclonal anti-human BRCA1 (16780 [ms110], Abcam), mouse monoclonal anti-mouse BRCA1 (sc287.17, Santa Cruz Biotechnology, 1:350), rabbit polyclonal anti-CREBBP (sc-369 [A-22], Santa Cruz Biotechnology), mouse monoclonal anti-HA (2367 [6E2], Cell Signaling Technology), mouse monoclonal anti-HIP1 (Rao et al., 2002)), rabbit polyclonal anti-TUBULIN (2144, Cell Signaling Technology, 1:5,000), rabbit polyclonal anti-VINCULIN (E1E9V, Cell Signaling Technology, 1:10,000).

Statistical Analysis. All statistical analysis was made using GraphPad Prism 6 software (GraphPad Software, Inc.). All data represent mean ±SD or SEM.

Supplemental References

Chan, W.I., Hannah, R.L., Dawson, M.A., Pridans, C., Foster, D., Joshi, A., Gottgens, B., Van Deursen, J.M., and Huntly, B.J. (2011). The transcriptional coactivator Cbp regulates self-renewal and differentiation in adult hematopoietic stem cells. Mol Cell Biol *31*, 5046-5060.

Foley, S.B., Hildenbrand, Z.L., Soyombo, A.A., Magee, J.A., Wu, Y., Oravecz-Wilson, K.I., and Ross, T.S. (2013). Expression of BCR/ABL p210 from a knockin allele enhances bone marrow engraftment without inducing neoplasia. Cell Rep *5*, 51-60.

Georgiades, P., Ogilvy, S., Duval, H., Licence, D.R., Charnock-Jones, D.S., Smith, S.K., and Print, C.G. (2002). VavCre transgenic mice: a tool for mutagenesis in hematopoietic and endothelial lineages. Genesis *34*, 251-256.

Kang-Decker, N., Tong, C., Boussouar, F., Baker, D.J., Xu, W., Leontovich, A.A., Taylor, W.R., Brindle, P.K., and van Deursen, J.M. (2004). Loss of CBP causes T cell lymphomagenesis in synergy with p27Kip1 insufficiency. Cancer Cell *5*, 177-189.

Kasper, L.H., Fukuyama, T., Biesen, M.A., Boussouar, F., Tong, C., de Pauw, A., Murray, P.J., van Deursen, J.M., and Brindle, P.K. (2006). Conditional knockout mice reveal distinct functions for the global transcriptional coactivators CBP and p300 in T-cell development. Mol Cell Biol *26*, 789-809.

Kung, A.L., Rebel, V.I., Bronson, R.T., Ch'ng, L.E., Sieff, C.A., Livingston, D.M., and Yao, T.P. (2000). Gene dose-dependent control of hematopoiesis and hematologic tumor suppression by CBP. Genes Dev *14*, 272-277.

Liu, Y., Wang, L., Han, R., Beier, U.H., Akimova, T., Bhatti, T., Xiao, H., Cole, P.A., Brindle, P.K., and Hancock, W.W. (2014). Two histone/protein acetyltransferases, CBP and p300, are indispensable for Foxp3+ T-regulatory cell development and function. Mol Cell Biol *34*, 3993-4007.

McCarthy, A., Savage, K., Gabriel, A., Naceur, C., Reis-Filho, J.S., and Ashworth, A. (2007). A mouse model of basal-like breast carcinoma with metaplastic elements. J Pathol *211*, 389-398.

Mgbemena, V.E., Signer, R.A., Wijayatunge, R., Laxson, T., Morrison, S.J., and Ross, T.S. (2017). Distinct Brca1 Mutations Differentially Reduce Hematopoietic Stem Cell Function. Cell Rep *18*, 947-960.

Rao, D.S., Hyun, T.S., Kumar, P.D., Mizukami, I.F., Rubin, M.A., Lucas, P.C., Sanda, M.G., and Ross, T.S. (2002). Huntingtin-interacting protein 1 is overexpressed in prostate and colon cancer and is critical for cellular survival. J Clin Invest *110*, 351-360.

Rebel, V.I., Kung, A.L., Tanner, E.A., Yang, H., Bronson, R.T., and Livingston, D.M. (2002). Distinct roles for CREB-binding protein and p300 in hematopoietic stem cell self-renewal. Proc Natl Acad Sci U S A *99*, 14789-14794.

Xu, W., Fukuyama, T., Ney, P.A., Wang, D., Rehg, J., Boyd, K., van Deursen, J.M., and Brindle, P.K. (2006). Global transcriptional coactivators CREB-binding protein and p300 are highly essential collectively but not individually in peripheral B cells. Blood *107*, 4407-4416.

Zhou, T., Perez, S.N., Cheng, Z., Kinney, M.C., Lemieux, M.E., Scott, L.M., and Rebel, V.I. (2016). Context Matters: Distinct Disease Outcomes as a Result of Crebbp Hemizygosity in Different Mouse Bone Marrow Compartments. PLoS One *11*, e0158649.

Zimmer, S.N., Lemieux, M.E., Karia, B.P., Day, C., Zhou, T., Zhou, Q., Kung, A.L., Suresh, U., Chen, Y., Kinney, M.C.*, et al.* (2012). Mice heterozygous for CREB binding protein are hypersensitive to gamma-radiation and invariably develop myelodysplastic/myeloproliferative neoplasm. Exp Hematol *40*, 295-306 e295.

Zimmer, S.N., Zhou, Q., Zhou, T., Cheng, Z., Abboud-Werner, S.L., Horn, D., Lecocke, M., White, R., Krivtsov, A.V., Armstrong, S.A.*, et al.* (2011). Crebbp haploinsufficiency in mice alters the bone marrow microenvironment, leading to loss of stem cells and excessive myelopoiesis. Blood *118*, 69-79.